Fe(III) T_1 MRI probes containing phenolate or hydroxypyridine-appended triamine chelates and a coordination site for bound water

Roy Cineus,[1] Samira M. Abozeid,[2] Gregory E. Sokolow,[1] Joseph A. Spernyak,[3] Janet R. Morrow[1*]

1. Department of Chemistry, University at Buffalo, The State University of New York Amherst, NY 14260, United States
2. Department of Chemistry, Faculty of Science, Mansoura University, El-Gomhoria Street, 35516 Mansoura, Egypt
3. Department of Cell Stress Biology, Roswell Park Comprehensive Cancer Center, Buffalo, New York 14263, United States

* to whom correspondence should be addressed at: jmorrow@buffalo.edu

Abstract

Fe(III) complexes containing a triamine framework and phenolate or hydroxypyridine donors are characterized and studied as T_1 MRI probes. In contrast to most Fe(III) MRI probes of linear chelates reported to date, the ligands reported here are pentadentate to give six-coordinate complexes with a coordination site for an inner-sphere water. The crystal structure of the complex containing unsubstituted phenolate donors Fe(L1)Cl, shows a six-coordinate iron center and contains a chloride ligand that is displaced in water. Two additional derivatives are sufficiently water soluble for study as MRI probes including a complex with a hydroxypyridine group, Fe(L2), and a hydroxybenzoic acid group, Fe(L3). The pH-potentiometric titrations give protonation constants of 7.2 and 7.5 for Fe(L2) and Fe(L3), respectively, that are assigned to deprotonation of the bound water. Changes in the electronic absorbance spectra of the complexes as a function of pH are consistent with deprotonation of phenol pendants at acidic pH values. However, the inner-sphere water ligand of Fe(L2) and Fe(L3) does not exchange rapidly on the NMR time scale at pH 6.0 or 7.4 as shown by variable temperature ^{17}O NMR spectroscopy. The pH-dependent proton relaxivity profiles show a maximum in relaxivity at near neutral pH, suggesting that exchange of the protons of the bound water is an important contribution. Competitive binding studies with EDTA show effective stability constants for Fe(L2) and Fe(L3) at pH 7.4 with log K values of 21.1 and 20.5, respectively. These two complexes are kinetically inert in carbonate phosphate buffer at 37 ^{o}C for several hours but transfer iron to transferrin. Fe(L2) and Fe(L3) show enhanced contrast in T_1 weighted imaging studies in BALB/c mice. These studies show that Fe(L2) clears through mixed renal and hepatobiliary routes while Fe(L3) has a similar pharmacokinetic clearance profile as a macrocyclic Gd(III) contrast agent.

Introduction

High-spin Fe(III) complexes are under development as magnetic resonance imaging (MRI) contrast agents after a hiatus of many years, in large part due to the success of Gd(III) complexes in the clinic.[1, 2] Gd(III) complexes have been used for several decades as MRI contrast agents, but concerns have arisen over residual Gd(III) in patients.[3-5] While Gd(III) contrast agents that contain macrocyclic ligands are thought to be safer than those with linear chelates,[6] these concerns have nonetheless motivated the search for alternatives.[7-10] High-spin Fe(III) complexes are suitable for development as T_1 MRI contrast agents given their symmetric half-filled d-subshell and correspondingly long electronic relaxation times. Moreover, the human body has biological pathways that regulate iron to maintain homeostasis and limit bioaccumulation. There are, however, significant hurdles to overcome in the chemistry of Fe(III) based MRI probes including the propensity of Fe(III) six-coordinate complexes to have inner-sphere water ligands that exchange too slowly to contribute optimally to relaxivity[7, 11] and for these water ligands to form hydroxide or bridging oxide complexes at neutral pH which generally reduces the relaxivity of the probe.[2, 12, 13] As a result of these challenges, the number of Fe(III) complexes that have been reported for in vivo MRI studies remains limited.[2, 14]

Similar to gadolinium-based contrast agents, high spin Fe(III) complexes shorten the T_1 relaxation times of water protons through inner-sphere, second-sphere, and outer sphere water interactions.[10, 15, 16] Dipole-dipole relaxation mechanisms are dominant and these interactions are governed by several correlation times including the rotational correlation time (τ_r) of the paramagnetic complex in solution, the exchange rate of the coordinated water molecule ($k_{ex} = 1/\tau_m$), the distance of the paramagnetic metal ion and the protons of the coordinated water (r_{MH}), as well as the electronic relaxation times of the paramagnetic metal ion (τ_s).[17] However, Fe(III) complexes in contrast to Gd(III) or Mn(II) based contrast agents, may have electronic relaxation rates that are sufficiently rapid to limit relaxivity at clinical magnetic field strengths (1.5 to 3 T).[10] Electronic relaxation arises from fluctuations in zero-field splitting, and there are both static and transient contributions. Theoretical methods have been applied recently to study the variation in zero-field splitting parameters for different Fe(III) complexes.[18-20] Thus it is

important to explore ligands that impart different coordination geometries in high-spin Fe(III) complexes.

Fe(III) complexes that have been studied as MRI probes are dominated by those containing polyaminocarboxylate ligands. Hexadentate ligands such as ethylenediaminetetraacetic acid (EDTA) and cyclohexanediaminetetraacetic acid (CDTA) are frequently studied because they form seven coordinate complexes with high spin Fe(III) that have a rapidly exchanging water ligand, which facilitates the production of effective T_1 relaxation of water protons.[10, 16, 21] However, a recent study of the solution chemistry of this class of Fe(III) complexes and their derivatives has shown there are challenges that need to be addressed with this type of ligand scaffold.[16] The inner-sphere water ligand of these complexes may deprotonate to form μ-hydroxide or μ-oxo-bridged Fe(III) species at physiological pH, which significantly decreases their relaxivity. Moreover, the Fe(III)/Fe(II) redox potentials of these complexes typically fall inside the physiological window for redox cycling (0.1 V – 0.9 V) when considering biologically abundant ascorbate as reductant and peroxide as oxidant. An Fe(III)/Fe(II) reduction potential in this range could lead to reduction of Fe(III) to Fe(II) complexes in vivo and corresponding production of radical oxygen species upon reaction with peroxide. Introduction of phenolate donor groups to this ligand scaffold, improves the redox stability of the Fe(III) complexes formed from these type of ligands.[22] On the other hand, some applications rely on the redox properties of Fe(III)/Fe(II) for the development of agents that register inflammation by oxidation to an Fe(III) T_1 agent.[12, 23, 24] Several complexes studied as redox-responsive iron-based agents feature a trans-diaminocyclohexane scaffold appended with pyridyl or imidazole donor groups.[12, 13]

Fe(III) complexes of macrocyclic ligands featuring triazacyclononane (TACN) are a more recently developed class of T_1 MRI probe.[7] These macrocycles may be appended with hydroxypropyl or phosphonate groups.[25, 26] Six-coordinate Fe(III) complexes with two hydroxypropyl pendants have an inner-sphere water which does not undergo rapid exchange on the NMR time scale.[7, 26] Such hydroxypropyl groups may enhance second-sphere interactions in Fe(III) complexes or facilitate proton exchange contributions to relaxivity. MRI studies of these complexes in mice show promising contrast enhancements in T_1-weighted imaging studies.[7, 26] Recent reports of

macrocyclic Fe(III) complexes with tetraazamacrocyclic ligands lack an inner-sphere water and have lower r_1 relaxivity values[24, 27] than do the TACN complexes containing an inner-sphere water.

Fe(III) MRI probes that lack an inner-sphere water include a recently reported bis-complex of Fe(III) with deferasirox, one of the most commonly-used iron sequestering agent in thalassemic patients[28] and a tetrahedral self-assembled Fe(III) cage that has four Fe(III) centers.[29] The contribution from second-sphere interactions in these complexes is sufficient to produce strong T_1 contrast enhancement upon administration in mice. Finally, an early type of Fe(III) MRI probe has a diamino-scaffold appended with carboxylate and phenolate donors (HBED, N,N'-bis(2-hydroxybenzyl)ethylene diamine-N,N'diacetic acid) to give a six-coordinate complex lacking an inner-sphere water.[14] The HBED complexes have low r_1 relaxivity; however, hydroxyalkyl substituents on the phenols and phosphonate pendants have been added to increase second-sphere interactions and promote higher relaxivity.[30]

Our goal in these studies was to develop ligands that would stabilize high spin Fe(III) complexes, have good aqueous solubility and contain an open coordination site for an inner-sphere water to improve relaxivity. We choose to use phenolate groups as they are among the strongest donors for Fe(III) and also stabilize the trivalent state.[31, 32] Moreover, phenolate groups appear to inhibit dimerization of Fe(III) centers through μ-oxo bridges.[22] However, we found that the phenolate groups had to be modified given that the unsubstituted phenolate analog (Fe(L1)) is not very water soluble. To improve solubility, the phenol group was exchanged for a hydroxypyridine group (L2), or derivatized with a carboxylate group (L3). Finally, a triamine scaffold has the advantage of providing an additional site for further functionalization at the central nitrogen.

The solution chemistry of the Fe(III) complexes featured in this study are compared to Fe(III) complexes of triaza-macrocyclic ligands and to complexes with the well-studied diamine-based framework. As predicted, the Fe(III) complexes studied here are six-coordinate with an inner-sphere water ligand occupying the sixth coordination site. Water exchange rates and the pH dependence of relaxivity are studied to better understand the mechanism of proton relaxation for these complexes. The good

aqueous solubility of two of the Fe(III) complexes is promising and facilitates their study as MRI probes in healthy mice.

Scheme 1. Fe(III) complexes studied here with predominant speciation shown at pH = 7.0.

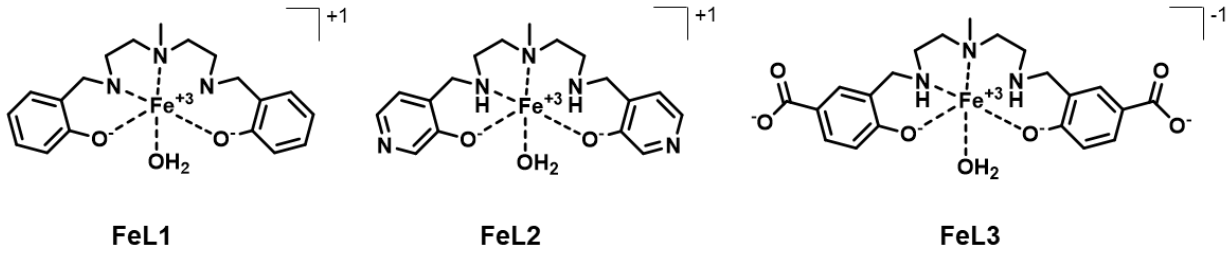

FeL1 **FeL2** **FeL3**

Results and Discussion

The ligands (L1-L3) were synthesized by using a reductive amination procedure, with sodium borohydride as the reducing agent.[33] First, a condensation reaction with N-methyl triamine, and two equivalents of salicylaldehyde (L1), 3-hydroxyisonicotinaldehyde (L2), or 3-formyl-4-hydroxybenzoic acid (L3) was carried out in methanol, then four equivalents of sodium borohydride were added to reduce the Schiff base. For L3, the Schiff-base was isolated prior to the reduction step, whereas for L1 and L2 the Schiff base was not isolated, but subsequently reduced in a one pot reaction. The Fe(III) complexes were synthesized by mixing the ligands with either ferric chloride or ferrous chloride in methanol or ethanol in the presence of triethylamine or potassium hydroxide as base. The Fe(III) complexes were isolated as chloride complexes. However in aqueous solutions of the complex, data is consistent with the chloride ligand being displaced by water in a process similar to six-coordinate Fe(III) macrocyclic complexes with a chloride ligand.[7] Treatment of aqueous solutions of Fe(L2) or Fe(L3) with $AgNO_3$ gives a quantitative precipitate of AgCl. Sequestration of the chloride ion does not change the proton relaxivity of the Fe(III) complexes within experimental error, consistent with hydrolysis of the complex to given an inner-sphere water upon dissolution of the complex (see Supporting Information).

The effective magnetic moments (μ_{eff}) were measured by using the Evans method in DMSO for Fe(L1) or in aqueous solutions for Fe(L2) and Fe(L3). The

corresponding effective magnetic moments of 6.0, 6.0 and 5.9, respectively, are consistent with high spin Fe(III) complexes. The spectroscopic data and synthetic procedures for the ligands and the Fe(III) complexes are given in the Supporting Information.

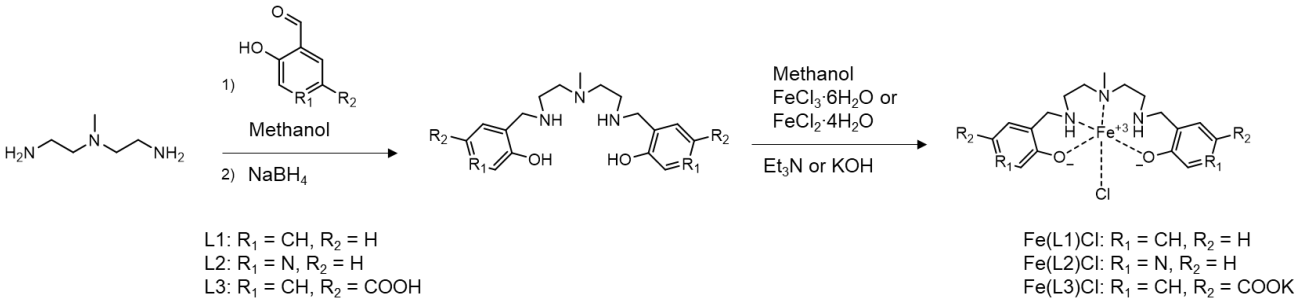

Scheme 2. Synthesis of L1, L2, and L3 and their Fe(III) complexes.

Structural characterization. Crystals of Fe(L1)Cl for x-ray diffraction studies were grown by slow evaporation of a concentrated acetonitrile solution over a period of one week. The Fe(III) center in this complex is coordinated to three amines and two phenolate groups from the N_3O_2 pentadentate ligand, with a chloride atom completing the coordination sphere. The triamine scaffold wraps around the Fe(III) center in a facial coordination mode. The central amine (N2) and one of terminal amines (N1) defines a plane with the Fe(III) center and the third amine forms a Fe-N bond which is nearly perpendicular to this plane. The phenolate groups (O1 & O2) are coordinated in a *cis*-configuration. To complete the coordination sphere, the chloride anion (Cl1) is coordinated in a *trans*-position to the terminal amine (N3). Hence, Fe(L1)Cl has a distorted octahedral geometry with bond angles deviating from the ideal values of 90° and 180°. Most notably, (O1-Fe1-N1) 170.7°, (O2-Fe1-Cl1) 100.3°, (O2-Fe1-N2) 160.7°, and (N3-Fe1-Cl1) 170.9°. In addition, the bond length between the iron(III) center and the chloride anion (2.342Å) is longer than the bond lengths of the other coordinated atoms: 1.923Å (Fe-O1), 1.908Å (Fe-O2), 2.255Å (Fe-N1), 2.195Å (Fe-N2), and 2.203Å (Fe-N3). The ORTEP representation of the crystal structure, is shown in Figure 1. The crystallographic data, bond lengths, and bond angles for [Fe(L1)Cl] are shown in Tables S6 – S8.

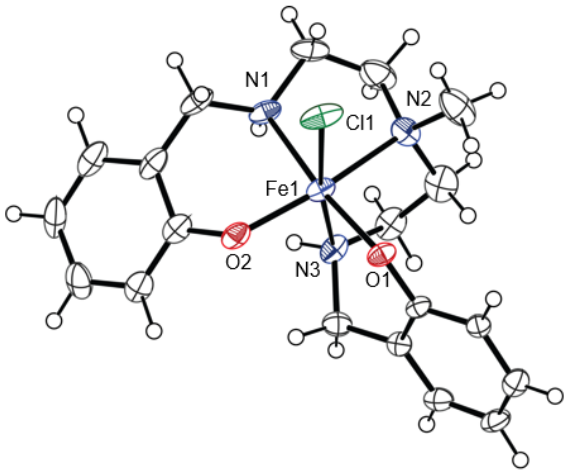

Figure 1. An ORTEP representation of the structure of [Fe(L1)Cl].

Stability and kinetic inertness of Fe(III) complexes. The stability of the Fe(III) complexes and their kinetic inertness towards dissociation was assessed for the two water soluble complexes, Fe(L2) and Fe(L3). The strong binding of Fe(III) to L2 and L3 even at low pH and the slow kinetics of Fe(III) complexation make the determination of stability constants from pH-potentiometric titrations challenging. Instead, a competing ligand method was used to obtain effective stability constants at near neutral pH. Fe(III) was titrated with L2 or L3 and with EDTA as a competing ligand, to determine the conditional formation constant (K_c), similar to previously reported examples.[31, 34] For each titration pH, Fe(III), and EDTA concentrations were kept constant, and the phenol-based ligand (L2 or L3) concentration was increased. Each batch titration was incubated for a week to ensure complete equilibration. A calibration curve for our Fe(III) complexes was constructed by using UV-Vis spectroscopy to determine the concentration of the Fe(III) complex for each titration (figures S25, 26) and mass balance equations (S4 – S6) were used to determine the other concentrations. The stability and protonation constants of Fe(EDTA) and EDTA ligand are given in Table S1[32] and used to determine the conditional stability constant of Fe(EDTA) at pH 7.4 as log K_c = 22.2 (eq S1 & S2). The K_{eq} determined from the competitive chelation of Fe(III) by L2 and L3 vs EDTA are 0.079 and 0.022, respectively (Figure S1). Hence, the log K_c for Fe(L2) and Fe(L3) at pH 7.4 are determined to be 21.1 and 20.5, respectively.

Table 1. Protonation constants for L2 and L3 and their Fe(III) complexes.

	L2	L3
$\log K_1^H$	9.8	11
$\log K_2^H$	8.7	9.1
$\log K_3^H$	6.8	7.2
$\log K_4^H$	3.6	4.3
$\log K_5^H$	–	3.3
$\log K_{FeL/FeL(OH)}^H$	7.2 (7.2)	7.5 (7.3)

Conditions for pH-potentiometric titrations: 1 mM of ligand or complex in 0.1 M KCl titrated with 0.1 M NaOH, 25°C. Values from UV-vis titrations (in parentheses) at 0.20 mM complex. Equilibrium expressions in SI (Table S3 - S5).

Stability constants of metal ion complexes correlate with the ligand basicity. Whereas the more basic ligand is expected to have the highest stoichiometric stability constant, the least basic ligand may have a higher effective stability constant at neutral or acidic pH. This is attributed to the competition with protons for the more strongly basic ligands which decreases the apparent stability constants.[35] A similar trend is observed for our Fe(III) complexes, although differences are modest. Protonation constants of our ligands (L2 and L3) determined using pH potentiometric titrations are shown in Table 1 and Figures S15 and S18. Comparison of the sum of the protonation constants (29 versus 32 for L2 and L3, respectively) suggests that L2 is less basic than L3. Here, the ionization assigned to the carboxylate group on L3 (K_5^H) is not included as it is not involved in coordination. Thus, the four-fold greater effective stability observed for Fe(L2) compared to Fe(L3) is consistent with L2 being less basic and more fully deprotonated at pH 7.4.

The protonation constants of the isolated Fe(III) complexes (Fe(L2)Cl and K_2[Fe(L3)Cl]) at neutral pH were determined by using pH potentiometric titrations over the range of pH 6-11 as shown in Figures S17 and S20 and Table 1. Data at acidic pH values was difficult to fit, most likely due to multiple equilibria and ionizations. Thus, additional information on the protonation of the Fe(III) complexes was collected by

monitoring their UV-vis spectra as a function of pH as discussed further below. Based on comparison to reports on similar complexes,[31, 32, 36] the protonation constants for Fe(L2) and Fe(L3) were assigned to specific groups.

The electronic absorbance spectra of the Fe(III) complexes of L2 and L3 were monitored as a function of pH as shown in Figures 2, S21-S27 to gain further insight into solution speciation. The spectra of the Fe(III) complexes at pH 7.4 show an intense LMCT band between 400 – 600 nm (Figure S28 and S29), which arises from the electronic transition between the lone pairs of the phenolate oxygens and the d-orbital manifold of the Fe(III) center.[37] The extinction coefficients for this LMCT band range from 3000 $M^{-1}cm^{-1}$ to 4000 $M^{-1}cm^{-1}$ for the two complexes, which is consistent with literature values.[38-42] For Fe(L2), a decrease in absorbance at 437 nm is observed with the concomitant increase of absorbance at ~550 nm upon increasing the pH from 3.6 to 8.9. In contrast, a more significant change in the electronic absorbance spectrum is observed for Fe(L3) upon variation of pH. At acidic pH, the intensity of the LMCT is diminished. Upon increasing the pH, the LMCT band becomes more intense, which we attribute to the deprotonation of the phenolate hydroxyl groups coordinated to the Fe(III). The LMCT undergoes a slight blue-shift at basic pH, which we attribute to the deprotonation of the coordinated water ligand. Detailed studies show that the LMCT peak at 436 nm for Fe(L2) and at 492 nm for Fe(L3) increases over the pH range of 2-3 and 3-4 to give protonation constants of log K = 2.3 and 3.7, respectively. Both curves were fit to two protonation events, consistent with both phenol pendants having similar values. For Fe(L3), we assume that the carboxylate groups undergo protonation at more acidic values. Fe(L2) shows an additional protonation with a log K of 5.2 which is assigned to protonation of the nitrogen moiety of one of the hydroxypyridine pendants (Figure S24). Absorbance peak intensities changes over the pH range of 6 to 8 for both Fe(L2) and FeL3) give log K values of 7.2 and 7.3, respectively which we assign to ionization of the bound water (Figure 2). These values match closely to those determined by pH potentiometric titrations. Thus we propose that the predominate species for Fe(L2) and Fe(L3 at physiological pH has both phenol groups deprotonated and a coordinated water/hydroxide ligand as shown in Scheme 1.

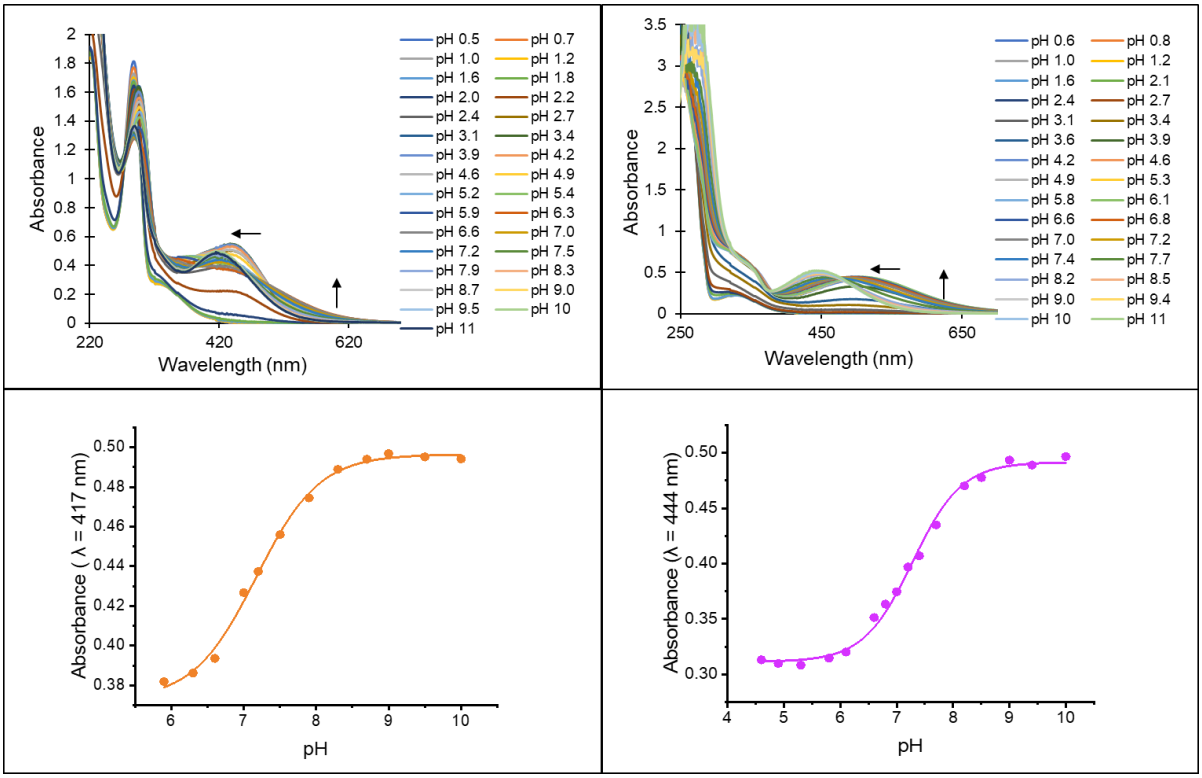

Figure 2. Spectrophotometric monitoring of pH titration of Fe(L2) and Fe(L3). Experimental Conditions: 0.10 M NaCl; pH adjusted with HCl(aq.) and NaOH(aq.), 25°C. Arrows show changes in the LMCT band as the pH is increased.

In addition to probing thermodynamic stability, it is of interest to study kinetic inertness to dissociation given its importance for MRI probes. The LMCT band of the Fe(III) complexes was monitored to study the kinetic inertness of the complexes under various conditions. The first study involved incubating the Fe(III) complexes in aqueous solutions of phosphate and carbonate ions at physiologically relevant concentrations. In this experiment, aqueous solutions containing 0.20 mM Fe(III) complex, 0.50 mM Na_2HPO_4 and 25 mM $NaHCO_3$ at pH 7.4 were incubated at 37°C over the course of 72 hours. There were no significant changes to the LMCT band over the course of 72 hours as shown in Figure S30 and S31. This shows that the complex remains intact under these conditions. It is also of interest to challenge the Fe(III) complexes against apo-transferrin, the iron transport protein in humans.[12, 23] Transferrin is a human glycoprotein which regulates iron homeostasis and has a high affinity for ferric ion with effective stability constants at pH 7.4 in serum bicarbonate of log K = 22.8 and 21.5,

respectively for the two different iron sites.[43, 44] Notably, these constants are one to two orders of magnitude larger than those of Fe(L2) and Fe(L3) at 21.1 and 20.5 at pH 7.4, respectively. An excess of transferrin (four-fold based on iron sites) was used to study first-order kinetics of trans-metalation. Aqueous solutions containing 0.05 mM Fe(III) complex and (0.10 mM) apo-transferrin at pH 7.4 were incubated at 37°C and monitored over the course of six hours. As shown in Figure S32 and S34, an exponential decrease in the absorbance of the complexes is observed within the first hour. The k_{obs} calculated for Fe(L2) and Fe(L3) are 0.037 min^{-1} ($t_{1/2}$ = 19 min) and 0.068 min^{-1} ($t_{1/2}$ = 10 min), respectively. Notably, this concentration of transferrin is 2-3 fold higher than that in the blood and transferrin sites already have fractional bound iron.[44] Experiments with a four-fold decrease in the concentration of transferrin produced transchelation of both Fe(III) complexes with a lowered rate constant of 0.015 min^{-1} ($t_{1/2}$ = 46 min) for Fe(L2) and 0.025 min^{-1} ($t_{1/2}$ = 28 min) (Figures S33, S35, S36).

To further test the stability or inertness of the complexes under biologically relevant conditions, Fe(L2) or Fe(L3) were incubated with mouse serum over 4 hours. The higher relaxivity that was observed in serum versus HSA suggests binding of the Fe(III) complexes to other serum proteins as we have observed previously for macrocyclic complexes of Fe(III).[26] The relaxivity of the Fe(L2) or Fe(L3) in serum did not change upon incubation over several hours (Figure 3). Notably, transferrin in blood is partially saturated with iron, so there would be reduced capacity for binding iron from the complexes. Alternatively, given that transferrin has a similar relaxivity as the complexes here,[22, 45] loss of iron from the complexes may not markedly change the apparent relaxivity.

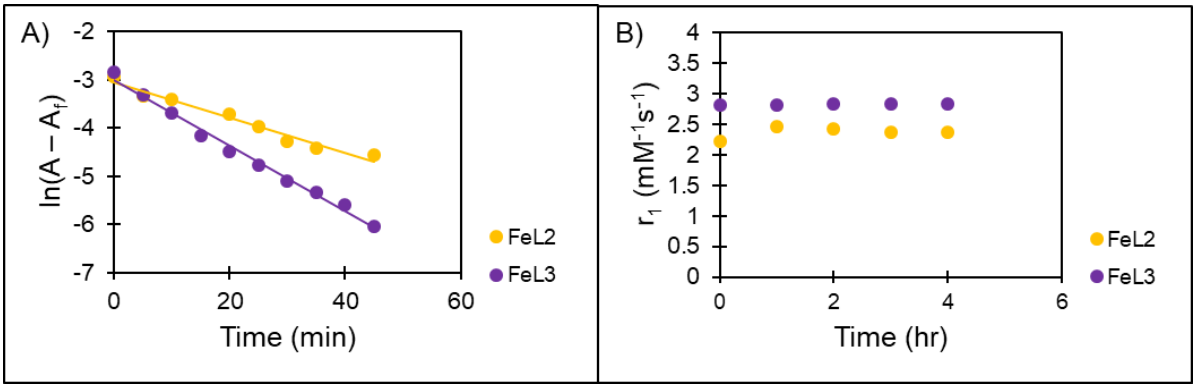

Figure 3. A) Rate constant determination of Fe transchelation for 0.050 mM Fe(L2) (yellow) and 0.050 mM Fe(L3) (purple) against 0.10 mM apo-transferrin. The slope represents the k_{obs} for Fe(L2) and Fe(L3) at 0.10 M NaCl,50 mM HEPES, 25 mM $NaHCO_3$, pH 7.4, 37°C. B) Relaxivity values of 0.20 mM FeL2 (yellow) and Fe(L3) (purple) in mouse serum over the course of 4 hours.

Electrochemical Measurements. The Fe(II)/Fe(III) redox potential of the Fe(L2) and Fe(L3) complexes was studied by using cyclic voltammetry in solutions containing 2 mM Fe(III) complex in 1.0 M KCl as the supporting electrolyte at pH 7.4. The cyclic voltammograms for Fe(L2) and Fe(L3) are shown in Figure S37. These data show that the reduction potentials (E1/2 ≈ E°) of Fe(L2) and Fe(L3) are -295 mV (-7.00 mV vs. NHE) and -395 mV (-107 mV vs NHE) respectively. The negative reduction potentials suggest that our Fe(III) complexes are likely to remain in the trivalent oxidation state in vivo as they are outside of the redox window of +0.1 V – +0.9V where iron complexes redox cycle in the presence of biological reductants and oxidants. This physiological window is estimated by the reduction potentials set by ascorbyl/monohydroascorbate couple and the hydrogen peroxide/water and hydroxide radical couple.[46]

^{17}O Water exchange experiments. Variable temperature ^{17}O NMR spectroscopy is a standard technique that is used to study exchange rates for water molecules that are directly coordinated to divalent or trivalent paramagnetic complexes containing Co(II), Fe(II), Mn(II), Fe(III), or Ln(III).[7, 25, 26, 29, 47-49] In these studies, the transverse relaxation rate of ^{17}O of water is measured in the presence or absence of the paramagnetic complex. As shown in Figure 4 the ^{17}O NMR transverse relaxivity (r_2^o) normalized to Fe(III) concentration for both complexes shows significantly less broadening compared to Fe(CDTA) which has a rapidly exchanging inner-sphere water

ligand, and similar the lack of broadening of Fe(DTPA) which lacks an inner-sphere water. However, the protonation constants of the Fe(III) water ligand is just below that of the pH of the experiments. For Fe(L2) most of the inner-sphere water is present as a bound hydroxide ligand that would not be expected to exchange. For Fe(L3) there should be roughly similar amounts of Fe(L3)(OH_2) and Fe(L3)(OH), but there is still no ^{17}O broadening, which is consistent with the bound water exchanging slowly on the NMR timescale. Experiments were also conducted under conditions where the inner-sphere water is proposed to be fully protonated for both complexes (pH = 6). A similar trend showing little line broadening was observed at pH 6 for both complexes (Figure S40). Therefore, we conclude that the inner-sphere water ligand does not exchange sufficiently fast on the NMR time scale to significantly broaden the ^{17}O NMR resonance, similar to macrocyclic complexes of Fe(III) we have reported.[7, 48] This lack of a rapidly exchanging water ligand is attributed to the strong Lewis acidity of the Fe(III) center in six-coordinate complexes.

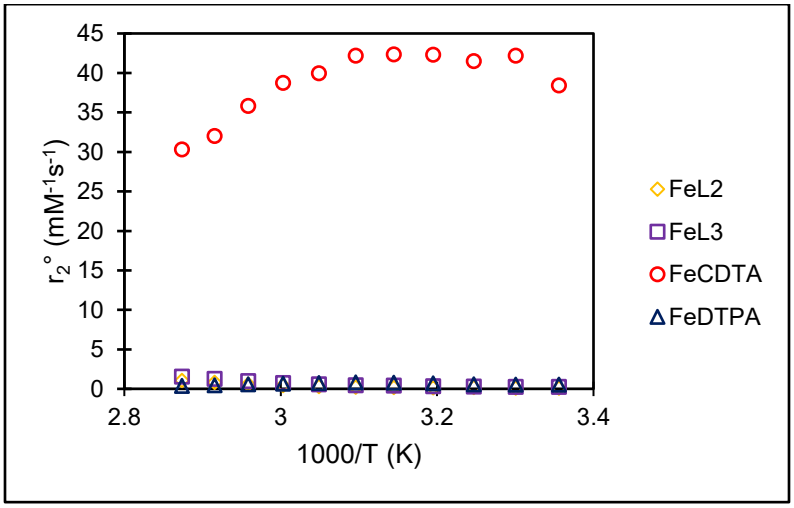

Figure 4. ^{17}O transverse relaxivity as a function of temperature at pH 7.4 for Fe(L2) and Fe(L3) compared to Fe(CDTA) and Fe(DTPA) at pH 6.5.

Proton relaxation times. The longitudinal proton relaxation times (T_1) for Fe(L2) and Fe(L3) were determined at 1.4 T (60 MHz) at 33 °C, pH 7.4. The transverse proton relaxation times (T_2) were measured by using multi-echo, Carr-Purcell-Meiboom-Gill spin-echo sequence. The linear fits of $1/T_1$ or $1/T_2$ versus concentration of complex to

give r_1 and r_2 are shown in Figure S38 & S39. The r_2/r_1 ratio for both Fe(III) complexes is close to 1 (Table 2), suggesting these Fe(III) complexes are suitable for development as T_1 MRI contrast agents. There were no significant changes in r_1 or r_2 relaxivity of Fe(L2) and Fe(L3) in the presence of human serum albumin (HSA) at 35 mg/mL (0.6 mM). The lack of an effect of HSA on relaxivity suggests that Fe(L2) and Fe(L3) do not bind to HSA and that the complexes will clear rapidly from the blood stream as extracellular agents. The larger r_1 relaxivity of Fe(L3) compared to Fe(L2) is consistent with the larger molecular size of Fe(L3) and a slower tumbling rate. In addition, the carboxylate groups may increase second-sphere water interactions.

The relaxivity of Fe(L2) and Fe(L3) can be compared to previously reported Fe(III) complexes that use linear chelators (Scheme 3 & Table 2).[16, 23, 30] The r_1 relaxivity for Fe(L2) and Fe(L3) are lower than other Fe(III) complexes with a rapidly exchangeable water, such as Fe(CDTA) or Fe(PyC3A). This further supports that fact the inner-sphere water for our Fe(III) complexes exchanges too slowly to contribute to the relaxivity via inner-sphere interactions. However, the relaxivity of our Fe(III) complexes is higher than Fe(III) complexes with no coordinated water, such as Fe(PDTA) or Fe(HBED). This suggests that the coordinated water of our Fe(III) complexes contributes to the relaxivity through second-sphere interactions or through proton exchange. All Fe(III) complexes show lower r_1 values compared to Gd(DOTA) (3.1 $mM^{-1}s^{-1}$) under similar conditions at 1.4 T.[50]

Table 2. Comparison of r_1 and r_2 relaxivity for Fe(L2) and Fe(L3) at 1.4 T, pH 7.4, 33 °C with analogous Fe(III) complexes.

Complex	**r_1 $mM^{-1}s^{-1}$**	**r_2 $mM^{-1}s^{-1}$**	**reference**
Fe(L2)	1.1± 0.1 (1.1± 0.1)	1.4 ± 0.1 (1.3 ± 0.1)	this work
Fe(L3)	1.5 ± 0.1 (1.5 ± 0.1)	1.8 ± 0.1 (1.7 ± 0.1)	this work
Fe(HBED)[a]	0.49	0.52	([30])
Fe(PDTA)[b]	0.66	-	([16])
Fe(CDTA)[c]	2.0[d]	2.2[d]	([21])
Fe(PyC3A)[d]	1.8	-	([23])

a. 40°C, b. 25°C (pH 5), c. 37 °C, 0.94T, d. 37 °C

Scheme 3. Chelating ligands used to form Fe(III) complexes as T_1 MRI probes.

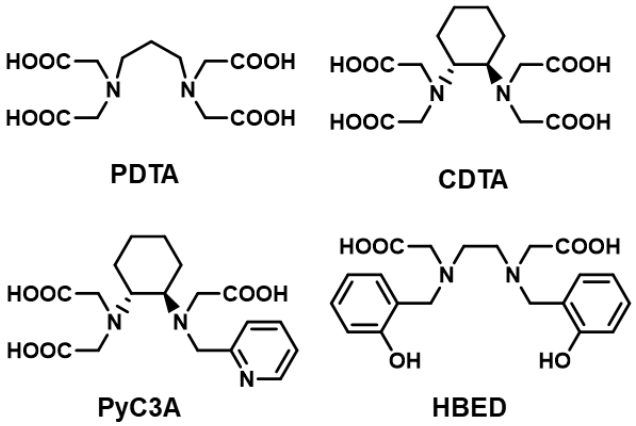

In order to further explore the mechanism of proton relaxation of our Fe(III) MRI probes, we measured relaxivity as a function of pH. The relaxivity was measured for solutions containing 0.2 mM of our Fe(III) complexes in 0.10 M HEPES and 0.10 M NaCl, taking care to subtract the relaxation rate of in the absence of iron complex under each condition. A separate set of experiments was conducted at 5 mM complex to determine whether the speciation of the complexes remains constant as a function of complex concentration as would be expected for mononuclear species. As shown in Figure 5, relaxivity increases with increasing pH between pH 4 and approximately 7.4. A decrease in relaxivity is observed upon increasing the pH from 7.4 to 11. This pH-relaxation profile differs from that reported for the Fe(III) complexes of EDTA derivatives that have relatively flat profiles from pH 3-6, then show a large decrease at pH values close to those of the pK_a values of bound water, most likely due to dimerization.[16]

One explanation for the increase in the relaxivity for Fe(L2) and Fe(L3) between pH 4 to 7.4 is base-catalyzed exchange of protons associated with the inner-sphere water. For certain Gd(III) probes, general base catalysis has been shown to be important in promoting exchange of the OH protons of hydroxy donor groups[51] but further studies with a range of general bases are needed here to distinguish this possibility from other postulates. The decrease in the r_1 relaxivity between pH 8 – 11 is attributed to the deprotonation of water ligand to give the Fe(L)OH species of lowered relaxivity, similar that observed for Fe(EDTA) and derivatives.[16] However, the relatively slight decrease in relativity for Fe(L2) or Fe(L3) in comparison to the Fe(EDTA) derivatives which form μ-oxo dimers is consistent with the lack of dimerization observed

for the complexes here. Even at relatively high concentrations of 5 mM, Fe(L2) and Fe(L3) appear to maintain mononuclear speciation as shown by the relaxivity versus pH curve which is similar to that at 0.20 mM complex (Fig. 5).

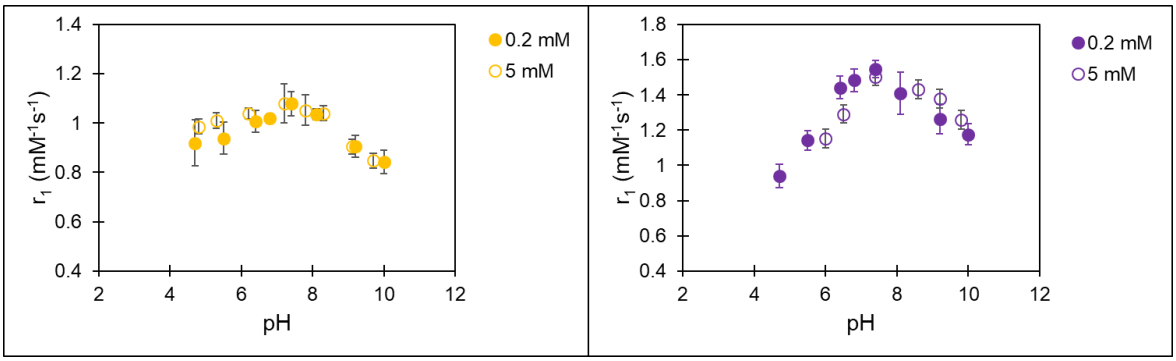

Figure 5. pH dependence of r_1 relaxivity for Fe(L2) (right) and Fe(L3) (left) at 1.4 T, 33°C.

MRI studies in mice. To further assess Fe(L2) or Fe(L3) as MRI probes, the complexes were injected into the tail vein of BALB/c mice at a of dose of 0.10 mmol/kg and monitored on a small animal 4.7 T MRI scanner. Data for mice at 10 min and 40 min post-injection with Fe(L2) (B &C) and Fe(L3) (E&F) are shown in Figure 6. A contrast enhancement of the kidneys can be observed at 10 min for both Fe(L2) and Fe(L3). At 40 min, the signal enhancement is prolonged for Fe(L2). However, the contrast enhancement from Fe(L3) is substantially decreased at 40 minutes consistent with more rapid clearance.

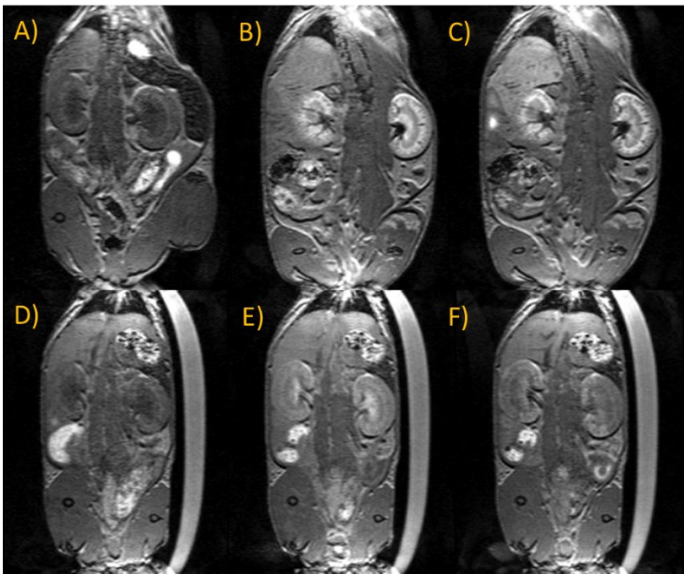

Figure 6. T_1–weighted MR images of BALB/c mice at 4.7 T upon injection with 0.10 mmol/kg Fe(L2) or Fe(L3). Top row: pre-injection (A), 10 min (B), and 40 min (C) post-injection images showing enhancement of kidneys for Fe(L2). Bottom row: pre-injection (D), 10 min (E), and 40 min (F) post-injection images showing enhancement of kidneys for Fe(L3).

Data shown in Figures S41 and 7 report on contrast enhancement in different organs over time to examine pharmacokinetic clearance. Comparison was made to Gd(DOTA) at the same dose. This data is consistent with Fe(L2) clearing through both the renal and hepatobiliary pathways, with significant signal enhancement in both the bladder and gallbladder at later time points. The clearance of Fe(L3) is predominately through the renal pathway, as enhancement is seen predominantly in the bladder by 15 minutes. Both Fe(L2) and Fe(L3), clear quickly from the vena cava (Figure S34) with signal enhancement that is about 50% less than that of Gd(DOTA). This is expected from the relative r_1 relaxivity of the iron complexes compared to the gadolinium complex in solution. The rapid clearance from the vena cava is also consistent with the in vitro relaxivity data which showed no significant enhancement in the presence of HSA (35mg/mL), which suggests that neither Fe(L2) nor Fe(L3) bind avidly to serum albumin.

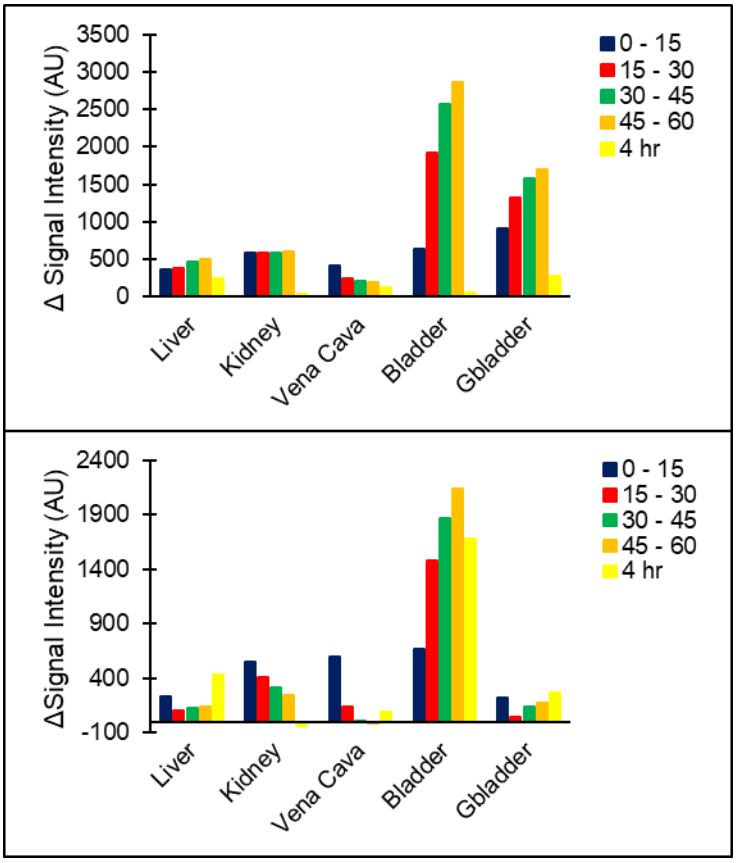

Figure 7. Changes in T_1 – weighted signal intensity observed in mice for Fe(L2) (top) and Fe(L3) (bottom) at 0.1 mmol/kg over time.

The prolonged contrast enhancement of Fe(L2) observed in the kidneys over four hours is reminiscent of cationic Fe(III) macrocyclic complexes we have reported.[7, 26] The prolonged enhancement of Fe(L2) observed in the liver is even more remarkable and suggests that this complex clears largely through the hepatobiliary pathway. Contrast agents have been developed for imaging the liver, but these are generally anionic complexes that are amphiphillic due to an appended aromatic group, often an ethoxy-benzyl group.[52] In contrast, Fe(L2) is a cationic complex with two heterocyclic pendants. Further studies are required to better understand this pharmacokinetic clearance profile. However the anionic complex, Fe(L3), clears from kidneys and liver with similar pharmacokinetics to that of Gd(DOTA) (Figure S41). This bodes well for the development of such complexes as alternatives to gadolinium-based contrast agents.

Conclusions

The ligands prepared in this study bind Fe(III) to form six-coordinate complexes with a coordination site for bound water as shown by x-ray crystallography and supported by solution studies. The structure and solution chemistry of the Fe(III) complexes studied here differs in several ways from previously studied complexes of linear chelates or macrocyclic ligands and allows us to elucidate the factors that are important in developing Fe(III) T_1 MRI probes. Advantages of these complexes include the stabilization of the Fe(III) center to produce redox potentials that are negative versus NHE. Moreover, the phenolate donors are easily functionalized to change the overall charge of the complex. The latter is important for influencing the biodistribution and clearance of the MRI probe in vivo. The complexes studied here have moderate water solubility (>10 mM), unlike some of the Fe(III) complexes we have developed for MRI applications.[7]

The inner-sphere water in Fe(L2) and Fe(L3) does not exchange rapidly on the NMR time scale and does not contribute to the proton relaxivity through the water exchange mechanism. However, the complexes show larger relaxivity than expected for Fe(III) complexes that lack an exchangeable inner-sphere water ligand. The pH dependence of the relaxivity has a maximum value at a pH where the phenols are deprotonated and the bound water is protonated. This suggests that the bound water contributes to relaxivity through proton exchange or through interaction with second-sphere waters. Further studies with buffers of different basicity may enable us to distinguish these possibilities and will be the subject of future studies. For example, Gd(III) contrast agents with hydroxyalkyl based OH donor groups undergo general-base catalyzed proton exchange as shown through experiments with buffers of different basicity.[49]

Another advantage of the Fe(III) complexes studied here is the apparent lack of formation of hydroxy-bridged dimers at neutral to basic pH that frequently occurs in Fe(III) complexes that have a bound water ligand. Formation of hydroxy-bridged dimers generally decreases the magnetic susceptibility of the Fe(III) centers through ferromagnetic coupling and results in insoluble complexes.[12, 13] The pH-relaxivity profile at different concentrations, pH potentiometric titrations and good solubility of the

complexes at basic pH all support the predominance of the mononuclear form of the complex under a wide range of conditions. Notably, a recently reported Fe(III) complex with a tetradentate chelate and two phenolates has bound water ligands, yet apparently does not form μ-hydroxy bridged dimers.[22]

The conditional stability constants at pH 7.4 of Fe(L2) and Fe(L3) are moderately large, although somewhat less than that of Fe(EDTA) or transferrin. As for kinetic properties, Fe(L2) and Fe(L3) are less inert than are the diamine-based hexadentate chelates, especially those containing a cyclohexyl group within the chelate.[23] The complexes studied here are also are substantially less inert to acidic conditions or to sequestration by transferrin compared to Fe(III) complexes of the tri-azamacrocyclic ligands with two or three pendent groups.[53] However, the differences in biodistribution and pharmacokinetic clearance of the Fe(L2) and Fe(L3) complexes suggests that transferrin does not sequester substantial iron from the complexes before they clear from the mice. This is consistent with recent studies showing that an Fe(III) complex that rapidly transfers iron to transferrin in solution does not completely dissociate iron when administered at 0.14 mmol/kg in mice but clears partially as intact complex. This is attributed to the saturation of iron bound transferrin in blood and its slow turnover.[22] Thus, while it is beneficial for contrast agents to clear from animals and remain largely intact, there may be advantages to the use of iron-based contrast agents if free iron is sequestered by transferrin.

Finally, the pharmacokinetics of clearance of the Fe(III) complexes compared to that of Gd(DOTA) is informative. Whereas the cationic Fe(L2) complex clears slowly through the hepatobiliary route and produces strong contrast enhancement in the liver and gall bladder, Fe(L3) shows a profile that is similar to that of Gd(DOTA). Pharmacokinetic clearance of Fe(L3) from the vena cava, liver and kidney is similar to that of Gd(DOTA), although the contrast enhancement is lower, consistent with the lower relaxivity of the Fe(L3) complex. This study illustrates a few of the factors that are important in the design of Fe(III) complexes to give MRI probes of high solubility, relaxivity and contrast enhancement in vivo.

Supporting Information.

Additional experimental details, materials, and methods including synthetic procedures and characterization of the ligands and Fe(III) complexes by NMR spectroscopy or mass spectrometry, pH potentiometric titrations; stability constants and kinetic inertness as monitored by changes in electronic spectra; proton relaxivity of iron complexes; pharmacokinetic data in mice and x-ray crystal structure data.

Acknowledgments.

JRM thanks the NSF (STTR-11951127and CHE-2004135) for support. JAS is partially supported by Roswell Park's NIH P30 grant (CA016056). R. C. acknowledges support by the National Institute of Health, National Institute of General Medical Science Award (R25 GM095459) to University at Buffalo. The authors would like to thank the Chemistry Instrument Center (CIC), University at Buffalo. This work utilized ICP-MS that was purchased with funding from a NSF Major Research Instrumentation Program (NSF CHE-0959565) and the Bruker 500 MHz NMR (NSF CHE-2018160).

Conflicts of Interest

JRM is cofounder of Ferric Contrast, a company that develops iron-based MRI contrast agents.

References

(1) Tweedle, M. F. Alternatives to Gadolinium-Based Contrast Agents. *Investig Radiol.* **2021**, *56* (1), 35-41.
(2) Kras, E. A.; Snyder, E. M.; Sokolow, G. E.; Morrow, J. R. Distinct Coordination Chemistry of Fe(III)-Based MRI Probes. *Acc Chem Res* **2022**, *55* (10), 1435-1444.
(3) Le Fur, M.; Caravan, P. The biological fate of gadolinium-based MRI contrast agents: a call to action for bioinorganic chemists. *Metallomics* **2019**, *11* (2), 240-254.
(4) Lancelot, E.; Raynaud, J. S.; Desche, P. Current and Future MR Contrast Agents Seeking a Better Chemical Stability and Relaxivity for Optimal Safety and Efficacy. *Investig Radiol* **2020**, *55* (9), 578-588.
(5) Kanal, E. Gadolinium based contrast agents (GBCA): Safety overview after 3 decades of clinical experience. *Magn Reson Imaging* **2016**, *34* (10), 1341-1345.
(6) Do, C.; DeAguero, J.; Brearley, A.; Trejo, X.; Howard, T.; Escobar, G. P.; Wagner, B. Gadolinium-Based Contrast Agent Use, Their Safety, and Practice Evolution. *Kidney360* **2020**, *1* (6), 561-568.
(7) Snyder, E. M.; Asik, D.; Abozeid, S. M.; Burgio, A.; Bateman, G.; Turowski, S. G.; Spernyak, J. A.; Morrow, J. R. A Class of FeIII Macrocyclic Complexes with Alcohol Donor Groups as Effective T1 MRI Contrast Agents. *Angew Chem Int Ed* **2020**, *59* (6), 2414-2419.
(8) Gupta, A.; Caravan, P.; Price, W. S.; Platas-Iglesias, C.; Gale, E. M. Applications for Transition-Metal Chemistry in Contrast-Enhanced Magnetic Resonance Imaging. *Inorg Chem* **2020**, *59* (10), 6648-6678.

(9) Botta, M.; Carniato, F.; Esteban-Gomez, D.; Platas-Iglesias, C.; Tei, L. Mn(II) compounds as an alternative to Gd-based MRI probes. *Future Med Chem* **2019**, *11* (12), 1461-1483.
(10) Baranyai, Z.; Carniato, F.; Nucera, A.; Horváth, D.; Tei, L.; Platas-Iglesias, C.; Botta, M. Defining the conditions for the development of the emerging class of FeIII-based MRI contrast agents. *Chem Sci* **2021**, *12* (33), 11138-11145.
(11) Schneppensieper, T.; Seibig, S.; Zahl, A.; Tregloan, P.; van Eldik, R. Influence of chelate effects on the water-exchange mechanism of polyaminecarboxylate complexes of iron(III). *Inorg Chem* **2001**, *40* (15), 3670-3676.
(12) Wang, H.; Cleary, M. B.; Lewis, L. C.; Bacon, J. W.; Caravan, P.; Shafaat, H. S.; Gale, E. M. Enzyme Control Over Ferric Iron Magnetostructural Properties. *Angew Chem Int Ed* **2022**, *61* (3), e202114019.
(13) Wang, H.; Wong, A.; Lewis, L. C.; Nemeth, G. R.; Jordan, V. C.; Bacon, J. W.; Caravan, P.; Shafaat, H. S.; Gale, E. M. Rational Ligand Design Enables pH Control over Aqueous Iron Magnetostructural Dynamics and Relaxometric Properties. *Inorg Chem* **2020**, *59* (23), 17712-17721.
(14) Kuznik, N.; Wyskocka, M. Iron(III) Contrast Agent Candidates for MRI: a Survey of the Structure-Effect Relationship in the Last 15 Years of Studies. *Eur J Inorg Chem* **2016**, (4), 445-458.
(15) Wahsner, J.; Gale, E. M.; Rodríguez-Rodríguez, A.; Caravan, P. Chemistry of MRI Contrast Agents: Current Challenges and New Frontiers. *Chem Rev* **2019**, *119* (2), 957-1057.
(16) Uzal-Varela, R.; Lucio-Martínez, F.; Nucera, A.; Botta, M.; Esteban-Gómez, D.; Valencia, L.; Rodríguez-Rodríguez, A.; Platas-Iglesias, C. A systematic investigation of the NMR relaxation properties of Fe(iii)-EDTA derivatives and their potential as MRI contrast agents. *Inorg Chem Front* **2023**, *10* (5), 1633-1649.
(17) Lauffer, R. B. Paramagnetic metal complexes as water proton relaxation agents for NMR imaging: theory and design. *Chem Rev* **1987**, *87* (5), 901-927.
(18) Mathies, G.; Blok, H.; Disselhorst, J. A. J. M.; Gast, P.; van der Meer, H.; Miedema, D. M.; Almeida, R. M.; Moura, J. J. G.; Hagen, W. R.; Groenen, E. J. J. Continuous-wave EPR at 275GHz: Application to high-spin Fe3+ systems. *J Magn Reson* **2011**, *210* (1), 126-132.
(19) Azarkh, M.; Groenen, E. J. J. Simulation of multi-frequency EPR spectra for a distribution of the zero-field splitting. *Journal of Magnetic Resonance* **2015**, *255*, 106-113.
(20) Mathies, G.; Gast, P.; Chasteen, N. D.; Luck, A. N.; Mason, A. B.; Groenen, E. J. Exploring the Fe(III) binding sites of human serum transferrin with EPR at 275 GHz. *J Biol Inorg Chem* **2015**, *20* (3), 487-496.
(21) Boehm-Sturm, P.; Haeckel, A.; Hauptmann, R.; Mueller, S.; Kuhl, C. K.; Schellenberger, E. A. Low-Molecular-Weight Iron Chelates May Be an Alternative to Gadolinium-based Contrast Agents for T1-weighted Contrast-enhanced MR Imaging. *Radiology* **2018**, *286* (2), 537-546.
(22) Sargun, A.; Fisher, A. L.; Wolock, A. S.; Phillips, S.; Sojoodi, M.; Khanna, S.; Babitt, J. L.; Gale, E. M. A Rationally Designed Complex Replenishes the Transferrin Iron Pool Directly and with High Specificity. *J Am Chem Soc* **2023**, *145* (12), 6871-6879.
(23) Wang, H.; Jordan, V. C.; Ramsay, I. A.; Sojoodi, M.; Fuchs, B. C.; Tanabe, K. K.; Caravan, P.; Gale, E. M. Molecular Magnetic Resonance Imaging Using a Redox-Active Iron Complex. *J Am Chem Soc* **2019**, *141* (14), 5916-5925.
(24) Karbalaei, S.; Franke, A.; Jordan, A.; Rose, C.; Pokkuluri, P. R.; Beyers, R. J.; Zahl, A.; Ivanovic-Burmazovic, I.; Goldsmith, C. R. A Highly Water- and Air-Stable Iron-Containing MRI Contrast Agent Sensor for H2O2. *Chem-Eur J* **2022**, *28* (46). DOI: ARTN e20220117910.1002/chem.202201179.

(25) Kras, E. A.; Abozeid, S. M.; Eduardo, W.; Spernyak, J. A.; Morrow, J. R. Comparison of phosphonate, hydroxypropyl and carboxylate pendants in Fe(III) macrocyclic complexes as MRI contrast agents. *J Inorg Biochem* **2021**, *225*, 111594.

(26) Asik, D.; Smolinski, R.; Abozeid, S. M.; Mitchell, T. B.; Turowski, S. G.; Spernyak, J. A.; Morrow, J. R. Modulating the Properties of Fe(III) Macrocyclic MRI Contrast Agents by Appending Sulfonate or Hydroxyl Groups. *Molecules* **2020**, *25* (10), 2291.
(27) Kadakia, R. T.; Ryan, R. T.; Cooke, D. J.; Que, E. L. An Fe complex for F-19 magnetic resonance-based reversible redox sensing and multicolor imaging. *Chem Sci* **2023**, *14* (19), 5099-5105.
(28) Palagi, L.; Di Gregorio, E.; Costanzo, D.; Stefania, R.; Cavallotti, C.; Capozza, M.; Aime, S.; Gianolio, E. Fe(deferasirox)2: An Iron(III)-Based Magnetic Resonance Imaging T1 Contrast Agent Endowed with Remarkable Molecular and Functional Characteristics. *J Am Chem Soc* **2021**, *143* (35), 14178-14188.

(29) Sokolow, G. E.; Crawley, M. R.; Morphet, D. R.; Asik, D.; Spernyak, J. A.; McGray, A. J. R.; Cook, T. R.; Morrow, J. R. Metal−Organic Polyhedron with Four Fe(III) Centers Producing Enhanced T1 Magnetic Resonance Imaging Contrast in Tumors. *Inorg Chem* **2022**, *61* (5), 2603-2611.
(30) Bales, B. C.; Grimmond, B.; Johnson, B. F.; Luttrell, M. T.; Meyer, D. E.; Polyanskaya, T.; Rishel, M. J.; Roberts, J. Fe-HBED Analogs: A Promising Class of Iron-Chelate Contrast Agents for Magnetic Resonance Imaging. *Contrast Media & Molecular Imaging* **2019**, *2019*, 8356931.
(31) Harris, W. R.; Motekaitis, R. J.; Martell, A. E. New multidentate ligands. XVII. Chelating tendencies of N-(o-hydroxybenzyl)iminodiacetic acid (H3L). *Inorg Chem* **1975**, *14* (5), 974-978.
(32) Ma, R.; Motekaitis, R. J.; Martell, A. E. Synthesis of N-hydroxybenzylethylenediamine-N,N′,N′-triacetic acid and the stabilities of its complexes with divalent and trivalent metal ions. *Inorg Chim Acta* **1995**, *233* (1), 137-143.
(33) Abdel-Magid, A. F.; Carson, K. G.; Harris, B. D.; Maryanoff, C. A.; Shah, R. D. Reductive Amination of Aldehydes and Ketones with Sodium Triacetoxyborohydride. Studies on Direct and Indirect Reductive Amination Procedures1. *The J Org Chem* **1996**, *61* (11), 3849-3862.
(34) Harris, W. R.; Raymond, K. N.; Weitl, F. L. Ferric ion sequestering agents. 6. The spectrophotometric and potentiometric evaluation of sulfonated tricatecholate ligands. *J Am Chem Soc* **1981**, *103* (10), 2667-2675.
(35) Ramakrishnam Raju, M. V.; Wilharm, R. K.; Dresel, M. J.; McGreal, M. E.; Mansergh, J. P.; Marting, S. T.; Goodpaster, J. D.; Pierre, V. C. The Stability of the Complex and the Basicity of the Anion Impact the Selectivity and Affinity of Tripodal Gadolinium Complexes for Anions. *Inorg Chem* **2019**, *58* (22), 15189-15201.
(36) Di Bernardo, P.; Zanonato, P. L.; Tamburini, S.; Tomasin, P.; Vigato, P. A. Complexation behaviour and stability of Schiff bases in aqueous solution. The case of an acyclic diimino(amino) diphenol and its reduced triamine derivative. *Dalton Trans* **2006**, (39), 4711-4721.
(37) Dean, R. K.; Fowler, C. I.; Hasan, K.; Kerman, K.; Kwong, P.; Trudel, S.; Leznoff, D. B.; Kraatz, H.-B.; Dawe, L. N.; Kozak, C. M. Magnetic, electrochemical and spectroscopic properties of iron(iii) amine–bis(phenolate) halide complexes. *Dalton Trans* **2012**, *41* (16), 4806-4816.
(38) Velusamy, M.; Palaniandavar, M.; Gopalan, R. S.; Kulkarni, G. U. Novel Iron(III) Complexes of Tripodal and Linear Tetradentate Bis(phenolate) Ligands: Close Relevance to Intradiol-Cleaving Catechol Dioxygenases. *Inorg Chem* **2003**, *42* (25), 8283-8293.
(39) Templeton, D. M. *Molecular and Cellular Iron Transport*; Taylor & Francis Group LLC, 2005.
(40) Que, L.; Kolanczyk, R. C.; White, L. S. Functional models for catechol 1,2-dioxygenase. Structure, reactivity, and mechanism. *J Am Chem Soc* **1987**, *109* (18), 5373-5380.
(41) Cox, D. D.; Que, L. Functional models for catechol 1,2-dioxygenase. The role of the iron(III) center. *J Am Chem Soc* **1988**, *110* (24), 8085-8092.
(42) Cox, D. D.; Benkovic, S. J.; Bloom, L. M.; Bradley, F. C.; Nelson, M. J.; Que, L.; Wallick, D. E. Catecholate LMCT bands as probes for the active sites of nonheme iron oxygenases. *J Am Chem Soc* **1988**, *110* (7), 2026-2032.
(43) Harris, W. R.; Pecoraro, V. L. Thermodynamic Binding Constants for Gallium Transferrin. *Biochemistry* **1983**, *22* (2), 292-299.
(44) Aisen, P.; Leibman, A.; Zweier, J. Stoichiometric and site characteristics of the binding of iron to human transferrin. *J Biol Chem* **1978**, *253* (6), 1930-1937.
(45) Bertini, I.; Galas, O.; Luchinat, C.; Messori, L.; Parigi, G. A Theoretical-Analysis of the H-1 Nuclear Magnetic-Relaxation Dispersion Profiles of Diferric Transferrin. *J Phys Chem* **1995**, *99* (39), 14217-14222.
(46) Koppenol, W. H.; Hider, R. H. Iron and redox cycling. Do's and don'ts. *Free Radical Biology and Medicine* **2019**, *133*, 3-10.
(47) Caravan, P.; Ellison, J. J.; McMurry, T. J.; Lauffer, R. B. Gadolinium(III) Chelates as MRI Contrast Agents: Structure, Dynamics, and Applications. *Chem Revi* **1999**, *99* (9), 2293-2352.
(48) Gale, E. M.; Zhu, J.; Caravan, P. Direct Measurement of the Mn(II) Hydration State in Metal Complexes and Metalloproteins through 17O NMR Line Widths. *J Am Chem Soci* **2013**, *135* (49), 18600-18608.
(49) Bond, C. J.; Sokolow, G. E.; Crawley, M. R.; Burns, P. J.; Cox, J. M.; Mayilmurugan, R.; Morrow, J. R. Exploring Inner-Sphere Water Interactions of Fe(II) and Co(II) Complexes of 12-Membered Macrocycles To Develop CEST MRI Probes. *Inorg Chem* **2019**, *58* (13), 8710-8719.

(50) Asik, D.; Abozeid, S. M.; Turowski, S. G.; Spernyak, J. A.; Morrow, J. R. Dinuclear Fe(III) Hydroxypropyl-Appended Macrocyclic Complexes as MRI Probes. *Inorg Chem* **2021**, *60* (12), 8651-8664.
(51) Aime, S.; Baranyai, Z. How the catalysis of the prototropic exchange affects the properties of lanthanide(III) complexes in their applications as MRI contrast agents. *Inorg Chim Acta* **2022**, *532*. DOI: ARTN 12073010.1016/j.ica.2021.120730.

(52) McRae, S. W.; Cleary, M.; DeRoche, D.; Martinez, F. M.; Xia, Y.; Caravan, P.; Gale, E. M.; Ronald, J. A.; Scholl, T. J. Development of a Suite of Gadolinium-Free OATP1-Targeted Paramagnetic Probes for Liver MRI. *J Med Chem* **2023**, *66* (10), 6567-6576.
(53) Kras, E. A. Iron(III) complexes as T1 MRI agents. Ph.D. Thesis: University at Buffalo, the State University of New York, Buffalo, NY, September 2023.